
Radiation Characteristics of Tunable Graphennas in the Terahertz Band

Ignacio LLATSER¹, Christian KREMERS², Dmitry N. CHIGRIN², Josep Miquel JORNET³,
Max C. LEMME⁴, Albert CABELLOS-APARICIO¹, Eduard ALARCÓN¹

¹Nanonetworking Center in Catalunya (N3Cat), Universitat Politècnica de Catalunya, Barcelona, Spain

²Theoretical Nano-Photonics Group, Institute of High-Frequency and Communication Technology, Faculty of Electrical, Information and Media Engineering, University of Wuppertal, D-42119 Wuppertal, Germany

³Broadband Wireless Networking Laboratory, School of Electrical and Computer Engineering, Georgia Institute of Technology, Atlanta, Georgia 30332, USA

⁴School of Information and Communication Technology, KTH Royal Institute of Technology, 16640 Kista, Sweden

⁵Department of Electrical Engineering and Computer Science, University of Siegen, 57076 Siegen, Germany

{llatser,acabello}@ac.upc.edu, {kremers,chigrin}@uni-wuppertal.de, jmjornet@ece.gatech.edu, lemme@kth.se, eduard.alarcon@upc.edu

Abstract. *Graphene-enabled wireless communications constitute a novel paradigm which has been proposed to implement wireless communications among nanosystems. Indeed, graphene-based plasmonic nano-antennas, or graphennas, just a few micrometers in size have been predicted to radiate electromagnetic waves at the terahertz band. In this work, the important role of the graphene conductivity in the characteristics of graphennas is analyzed, and their radiation performance both in transmission and reception is numerically studied. The resonance frequency of graphennas is calculated as a function of their length and width, both analytically and by simulation. Moreover, the influence of a dielectric substrate with a variable size, and the position of the patch with respect to the substrate is also evaluated. Further, important properties of graphene, such as its chemical potential or its relaxation time, are found to have a profound impact in the radiation properties of graphennas. Finally, the radiation pattern of a graphenna is compared to that of an equivalent metallic antenna. These results will prove useful for designers of future graphennas, which are expected to enable wireless communications among nanosystems.*

Keywords

Graphenna, graphene-based plasmonic nano-antenna, graphene, terahertz, resonant frequency, Surface Plasmon Polariton.

1. Introduction

Graphene, a flat monoatomic layer of carbon atoms densely packed in a two-dimensional honeycomb lattice, has recently attracted the attention of the research community

due to its novel mechanical, thermal, chemical, electronic and optical properties [1, 2, 3]. Due to its unique characteristics, graphene has given rise to a plethora of potential applications in many diverse fields, ranging from ultra high-speed transistors [4] to transparent solar cells [5].

Among these, a particularly promising emerging field is graphene-enabled wireless communications. Wireless communications among nanosystems cannot be achieved by simply reducing the size of a classical metallic antenna down to a few micrometers, since that would impose the use of very high resonant frequencies, in the optical range. Due to the expectedly very limited power of nanosystems, the low mobility of electrons in metals when nanoscale structures are considered, and the challenges in implementing optical nano-transceivers, the feasibility of wireless communications among nanosystems would be compromised if this approach were followed. However, due to its groundbreaking properties, graphene is seen as the enabling technology to implement wireless communications among nanosystems. Indeed, graphene-based plasmonic nano-antennas, or *graphennas*, just a few micrometers in size are envisaged to radiate electromagnetic waves in the terahertz band [6], at a dramatically lower frequency and with a higher radiation efficiency with respect to their metallic counterparts. Moreover, the progress in the development of graphene-based components shows that the high electron mobility of graphene makes it an excellent candidate for ultra-high-frequency applications [7]. Recently-published work demonstrates the great potential of graphene-based ambipolar devices for analog and RF circuits, such as LNAs, mixers and frequency multipliers [8, 9, 10, 11].

In consequence, graphennas have the potential to enable wireless communications among nanosystems, leading to a novel networking paradigm known as nanonetworking [12]. Nanonetworks will enhance the capabilities of indi-

vidual nanosystems both in terms of complexity and range of operation. As a result, by allowing a swarm of nanosystems to communicate and share information among them, they are envisaged to create new applications in diverse fields. For instance, in the biomedical field, nanonetworks will allow the implementation of technologies such as nanorobots [13], nanodiagnostic techniques [14] and cooperative drug delivery systems using nanoparticles [15], whose implementation requires a group of coordinated nanosystems to become reality.

In our previous work [16, 17], a graphenna was modeled as a rectangular graphene patch over a dielectric substrate (see Fig. 1). This model was used to obtain the resonant frequency of a graphenna both analytically and numerically. Further, our parametric study of the graphenna resonances [18] allowed evaluating the influence of several parameters on the resonant frequency of a graphenna. The considered parameters included the dimensions of the dielectric substrate supporting the graphene patch, and the position of the patch with respect to the substrate. Moreover, the radiation pattern of a graphenna was compared to that of an equivalent metallic antenna of the same dimensions.

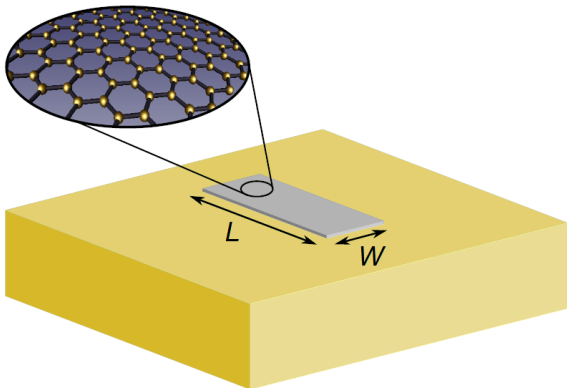


Fig. 1. Schematic diagram of a graphene-based plasmonic nano-antenna, or graphenna.

In this paper, we complete this analysis [18] by considering the influence of two key parameters of the graphene conductivity: the chemical potential and the relaxation time. We outline their importance and study their influence on both the graphene conductivity and the antenna resonances. These results will allow designers of future graphennas to select the appropriate parameters to optimize their radiation performance.

The rest of this paper is organized as follows. In Section 2, the unique properties of graphene for the propagation of Surface Plasmon Polariton waves, which constitute one of the main characteristics of graphennas, is outlined. Section 3 contains a parametric study of the resonant frequency of graphennas. The dependence of the graphenna resonances on the considered parameters is obtained by simulation, and guidelines for the design of future graphennas are given. In Section 4, the radiation pattern of a graphenna is compared to that of an equivalent metallic antenna. Finally, Section 5

concludes the paper.

2. Propagation of SPP Waves in Graphennas

Graphene presents excellent conditions for the propagation of Surface Plasmon Polaritons (SPP), electromagnetic waves guided along a metal-dielectric interface which are generated by an incident high-frequency radiation. Indeed, a free-standing graphene layer supports transverse-magnetic SPP waves with an effective mode index n_{eff} given by [19]

$$n_{\text{eff}}(\omega) = \sqrt{1 - 4 \frac{\mu_0}{\epsilon_0} \frac{1}{\sigma(\omega)^2}}. \quad (1)$$

where $\sigma(\omega)$ is the frequency-dependent graphene conductivity. It becomes then clear that, in order to model the propagation of SPP waves in graphennas, we first need to study the graphene conductivity. Analogously to our previous work [16, 17], since graphennas have an envisaged size in the order of a few micrometers, we disregard in this analysis the edge effects in the graphene conductivity. Therefore, the electrical conductivity model developed for infinite graphene sheets [20, 21] is used.

According to this model, the surface conductivity of an infinite graphene layer is calculated by means of the Kubo formalism. In the frequency region of interest (below 5 THz), the Drude-like intraband contribution dominates [22] and it is represented in a local form as follows:

$$\sigma(\omega) = \frac{2e^2}{\pi\hbar} \frac{k_B T}{\hbar} \ln \left[2 \cosh \left[\frac{\mu_c}{2k_B T} \right] \right] \frac{i}{\omega + i\tau^{-1}}, \quad (2)$$

where τ is the relaxation time, T is the temperature and μ_c is the chemical potential.

Once the graphene conductivity has been calculated, the propagation of SPP waves in graphennas can be studied. Indeed, in a graphenna, the edge of the graphene patch acts as a mirror and the graphenna behaves as a resonator for SPP modes. The coupling of the incident electromagnetic radiation with the corresponding SPP modes leads to resonances in the graphenna. The resonance condition is given by

$$m \frac{1}{2} \frac{\lambda}{n_{\text{eff}}} = L + 2\delta L \quad (3)$$

where m is an integer determining the order of the resonance, λ is the wavelength of the incident radiation, L is the graphenna length and δL is a measure of the field penetration outside the graphenna. This equation determines a set of m resonance frequencies ω_m corresponding to m modes of the resonator.

We consider graphennas with a size of a few micrometers, small enough so that they can be integrated into a

nanosystem. Since the effective mode index n_{eff} in graphene is in the order of 10^2 [19], according to this model, the first resonance frequency of graphennas lies in the terahertz band, around two orders of magnitude below what it would be expected in a metallic antenna with the same size. This fundamental difference constitutes one of the main reasons why graphennas are seen as the enabling technology for wireless communications among nanosystems. Next, the radiation properties of graphennas is further explored by means of a simulation-based parametric study of their resonant frequency.

3. Parametric Study of Graphennas

In this section, the dependence of the graphenna resonant frequency on several key parameters is analyzed. The size of the graphene patch, the dielectric substrate which supports it, the chemical potential of graphene and its relaxation time. The obtained results will allow deriving guidelines for the design of future graphennas.

3.1 Dimensions of the Graphene Patch

The model described in Section 2 can be used to estimate the spectral position of the resonances in a graphenna. Fig. 2 shows the position of the first resonance of a free-standing graphenna (without substrate) as a function of its length. The analytical expression, as obtained from the previous model, is compared with the results of numerical simulations done using the method of moments with surface equivalence principle [23].

In the simulations, the graphenna is modeled as a first approximation as an infinitely wide graphene patch with length $L = 5 \mu\text{m}$. Throughout the paper, the graphene conductivity is computed by assuming a relaxation time of $\tau = 10^{-13}\text{s}$, room temperature and zero chemical potential, unless otherwise specified. The excitation consists of a plane wave normally incident to the graphenna. Finally, the penetration length is set to $\delta L = 0.5 \mu\text{m}$. As it can be observed, the simulation results show a very good agreement with the analytical model.

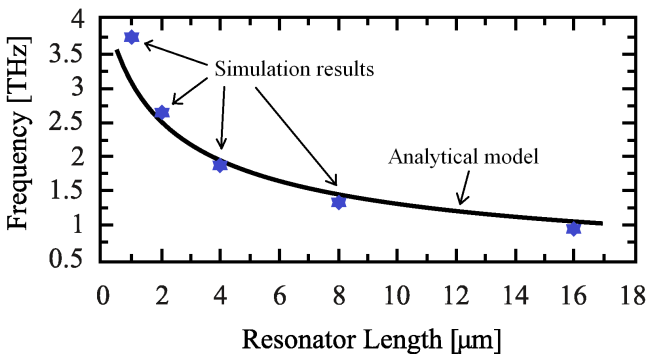


Fig. 2. Dependence of the first resonance of an infinitely wide graphenna as a function of its length. The solid line is as calculated using the analytical model and the stars correspond to the resonance frequencies obtained by simulation.

A realistic graphenna, however, will have a finite width. Fig. 3 shows the absorption cross section of a $5 \mu\text{m}$ -long graphenna, for different values of the antenna width, calculated by numerical simulation. The absorption cross section is a measure of the fraction of the power of the incident wave that is absorbed by the graphenna; therefore, the graphenna resonant frequency coincides with the frequency at which the absorption cross section is maximum. We can see in Fig. 3 that the resonant frequency is reduced as the graphenna becomes narrower.

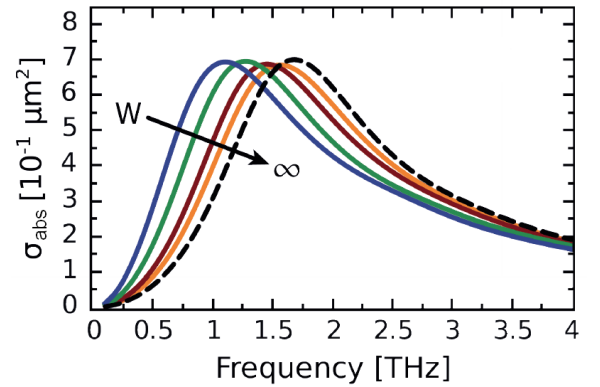


Fig. 3. Dependence of the absorption cross section of a graphenna as a function of its width. The absorption cross section normalized to the graphenna width is shown. The length of the graphenna is $L = 5 \mu\text{m}$. The plots correspond to infinite, $10 \mu\text{m}$, $5 \mu\text{m}$, $2 \mu\text{m}$ and $1 \mu\text{m}$ wide patches (right to left).

These results suggest that, by adjusting the dimensions of the graphenna (in particular its length), its radiation frequency can be tuned in a wide spectral range.

3.2 Dielectric Substrate

It is worth investigating the behavior of a graphenna when a more realistic model is used. With this purpose, we consider next a graphenna modeled as a graphene patch deposited on a dielectric substrate. In particular, we analyze the dependence of the antenna absorption cross section on the substrate size. We consider a graphenna composed of a graphene patch with a size of $5 \times 0.5 \mu\text{m}$, located on the center of a silicon substrate with a square shape and a thickness of $1 \mu\text{m}$. Fig. 4 shows the absorption cross section of the graphenna for different substrate sizes, from $6 \times 6 \mu\text{m}$ to infinity. On the one hand, it can be seen that a larger substrate improves the performance of the graphenna, since the absorption cross section increases with the substrate size, up to a given limit. On the other hand, the antenna resonant frequency is shown to be virtually constant at 0.5 THz , independently of the substrate size.

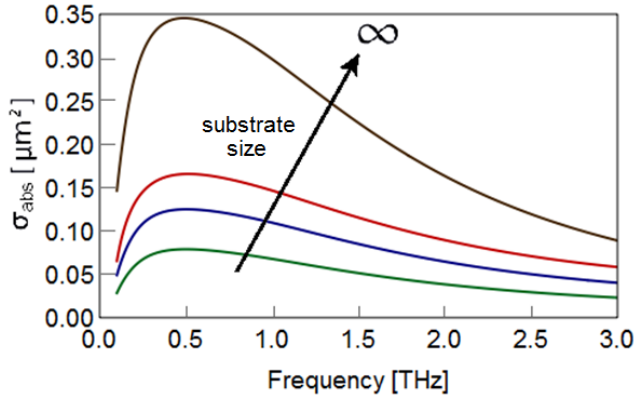


Fig. 4. Absorption cross section of a graphenna, for different substrate sizes: $6 \times 6 \mu\text{m}$, $10 \times 10 \mu\text{m}$, $16 \times 16 \mu\text{m}$ and infinite (below to above).

Next, we evaluate the influence of the position of the graphene patch relative to the substrate. The considered substrate has dimensions of $6 \times 6 \mu\text{m}$ and a thickness of $1 \mu\text{m}$. The graphene patch measures $5 \times 0.5 \mu\text{m}$ and is located in three different positions, as shown in Fig. 5: in the center of the substrate (5a), at $1.25 \mu\text{m}$ from the center (5b) and at $2.5 \mu\text{m}$ from the center (5c). Fig. 6 shows the antenna absorption cross section as a function of frequency, for each of these three configurations. As it can be observed, the absorption cross section increases as the graphene patch is located closer to the side of the substrate. Moreover, the resonant frequency becomes slightly higher when the patch is farther from the center.

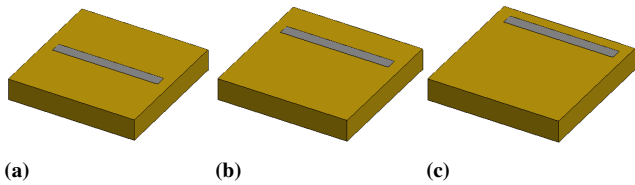


Fig. 5. Different positions of the graphene patch with respect to the substrate: patch in the center of the substrate (a), at $1.25 \mu\text{m}$ from the center (b) and at $2.5 \mu\text{m}$ from the center (c).

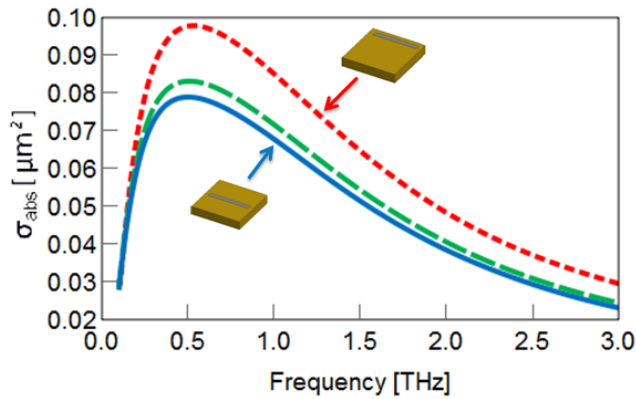


Fig. 6. Absorption cross section of a graphenna, for different positions of the graphene patch: in the center of the substrate (blue solid line), at $1.25 \mu\text{m}$ from the center (green dashed line) and at $2.5 \mu\text{m}$ from the center (red dotted line).

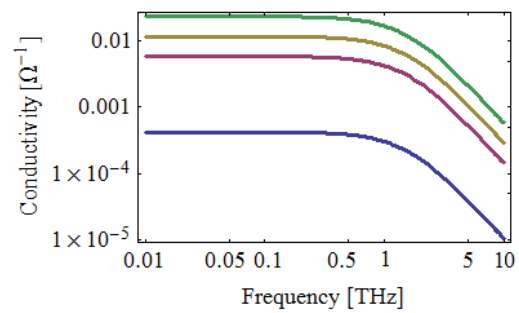
These results indicate that, on the one hand, as the dielectric substrate becomes larger, the power absorbed by the graphenna increases, up to a certain extent. On the other hand, for a given substrate size, the optimal location for on-chip graphennas may be near the edge of the substrate, in order to maximize their efficiency.

3.3 Chemical Potential

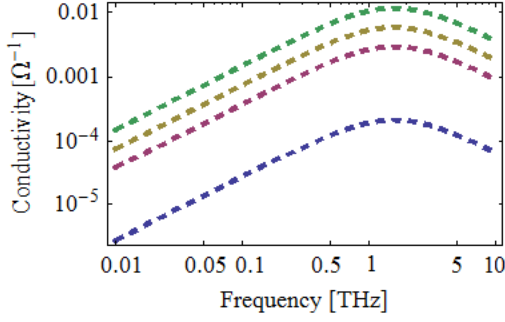
Another parameter of great interest to evaluate the performance of the graphenna is the chemical potential of the graphene patch, i.e., the level in the distribution of electron energies at which a quantum state is equally likely to be occupied or empty.

The results obtained so far in this study have assumed a model of graphene with zero chemical potential. However, as shown in Eq. (2), varying the chemical potential of graphene will affect the electrical conductivity of the graphenna, which is one of the main factors that determine its radiation performance. The chemical potential of graphene can be easily controlled by means of doping and/or by applying an electrostatic bias voltage, thereby allowing to dynamically tune the radiation properties of graphennas. We examine next how varying the chemical potential of graphene will impact the resonant frequency of graphennas.

Fig. 7a and 7b show the real and imaginary parts of the frequency-dependent graphene conductivity, respectively, calculated for different chemical potentials. A realistic range of values for the chemical potential, from 0 to 2 eV, has been chosen based on existing results in the literature [24, 25]. It can be observed that, by changing the chemical potential, the conductivity of graphene can be indeed controlled; in particular, increasing the chemical potential results in higher values of both the real and imaginary parts of the conductivity.



(a) Real part of the graphene conductivity



(b) Imaginary part of the graphene conductivity

Fig. 7. Log-log plots of the electrical conductivity of graphene as a function of the frequency, for different values of the chemical potential: 0 eV (blue line), 0.5 eV (purple line), 1 eV (yellow line) and 2 eV (green line).

Therefore, it can be expected that the graphene chemical potential will also affect the amount of power absorbed by the graphenna and, in consequence, its resonant frequency. Fig. 8 shows the absorption cross section of a graphenna as a function of frequency. The graphene conductivity models shown in Fig. 7, obtained varying the chemical potential from 0 to 2 eV, were considered. Moreover, the absorption cross section of a metallic antenna, modeled as a gold antenna with the same size as the graphenna and a thickness of 20 nm, is shown with a dashed gray line.

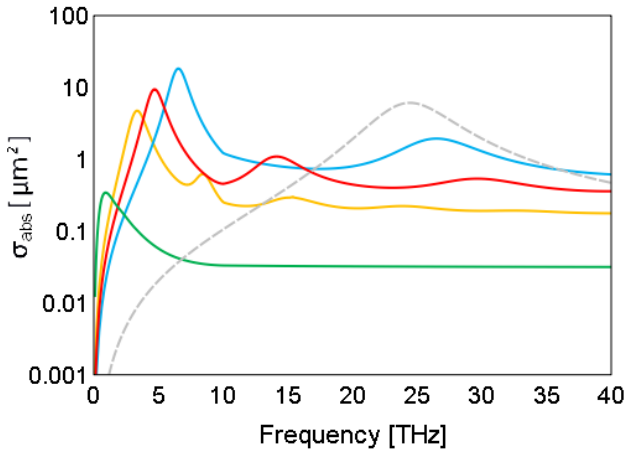


Fig. 8. Absorption cross section (in logarithmic scale) of a graphenna as a function of frequency, for different values of the chemical potential: 0 (green line), 0.5 (yellow line), 1 (red line) and 2 eV (blue line). The results are compared to that of an equivalent gold antenna with the same size (gray dashed line).

Indeed, as it can be observed, the maximum absorption cross section increases by a factor of 50 as the chemical potential changes from 0 to 2 eV. Furthermore, as shown in Table 1, the resonant frequency of the graphenna also changes dramatically when varying the chemical potential. However, in any case, the resonant frequencies of graphennas remain well below that of a metallic antenna with the same size.

Chemical potential	Resonant frequency
0 eV	0.918 THz
0.5 eV	3.356 THz
1 eV	4.704 THz
2 eV	6.541 THz

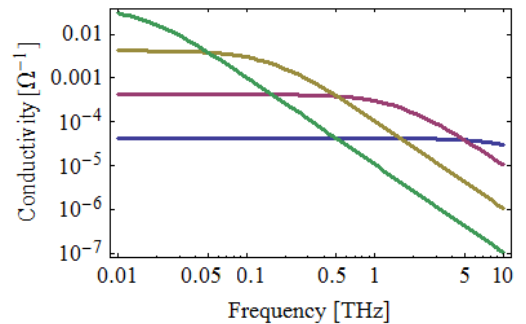
Table 1. Resonant frequency of a graphenna with length 5 μm and width 0.5 μm as a function of the chemical potential.

In summary, in terms of chemical potential, there is a trade-off between the amount of power that a graphenna can absorb and its resonant frequency. On the one hand, graphennas with zero chemical potential resonate at a low frequency but with a small absorption cross section, which will limit their achievable radiation efficiency. On the other hand, graphennas with a higher chemical potential possess greater absorption capabilities, but their resonant frequency also increases, which will reduce their potential transmission range. A compromise between these two magnitudes will therefore need to be reached by designers of future graphennas to implement wireless communications among nanosystems.

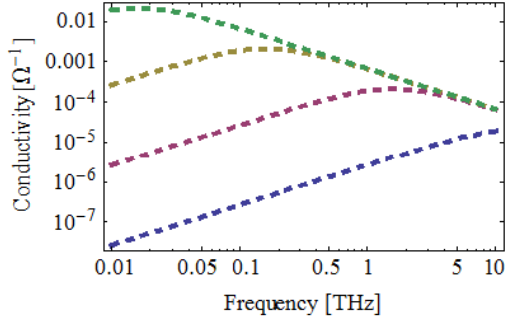
3.4 Relaxation Time

The relaxation time of a material is the time that it takes for a charge distortion as fluctuation to relax to a uniform charge density after it has been introduced in the material. The relaxation time in graphene depends, amongst others, on the quality of the graphene sample and it is a fundamental parameter of its conductivity model (2). In recent works, several authors consider different values for the relaxation time of graphene, ranging from 10^{-14} s to 10^{-11} s [26, 27, 28, 29]. Since there does not seem to exist a common agreement for the value of the relaxation time in graphene, we consider next its influence on the radiation properties of graphennas.

Fig. 9a and 9b show the real and imaginary parts of the frequency-dependent graphene conductivity, respectively, for different relaxation times based on values found in the literature [26, 27, 28, 29]. We can see that the relaxation time will have a strong influence on the graphene conductivity, whose value changes up to 3 orders of magnitude depending on the relaxation time.



(a) Real part of the graphene conductivity



(b) Imaginary part of the graphene conductivity

Fig. 9. Log-log plots of the electrical conductivity of graphene as a function of the frequency, for different values of the relaxation time: 10^{-14} s (blue line), 10^{-13} s (purple line), 10^{-12} s (yellow line) and 10^{-11} s (green line).

The absorption cross section of graphennas is shown in Fig. 10 for different relaxation times. Interestingly, the chosen value for the relaxation time τ has a huge impact on the resonant character of the graphenna and its bandwidth. In particular, for $\tau = 10^{-14}$ s, the graphenna does not resonate in the terahertz band. When $\tau = 10^{-13}$ s, a wide resonance around 1 THz is observed, with a -3 dB bandwidth of 1.9 THz. As the relaxation time continues to increase, higher-order resonances appear and a more intense resonant behavior is observed. Furthermore, the -3 dB bandwidth diminishes dramatically, to 0.16 THz in the case of $\tau = 10^{-12}$ s, and to 0.019 THz for $\tau = 10^{-11}$ s.

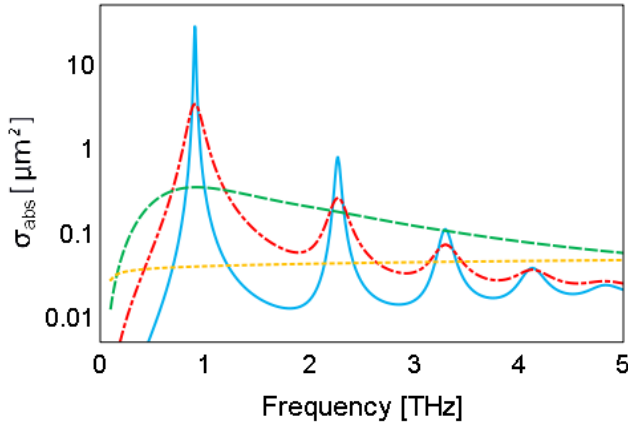


Fig. 10. Absorption cross section (in logarithmic scale) of a graphenna as a function of frequency, for different values of the relaxation time: 10^{-14} s (yellow dotted line), 10^{-13} s (green dashed line), 10^{-12} s (red dot-dashed line) and 10^{-11} s (blue solid line).

Given that the main application envisaged for graphennas consists of wireless communications among nanosystems, a bandwidth as large as possible is desired in order to maximize the channel capacity. Therefore, we conclude that the optimal value of the relaxation time for graphennas is around $\tau = 10^{-13}$ s, in order to achieve a resonant behavior while maintaining a radiation bandwidth as large as possible.

4. Radiation Pattern

Finally, we study the properties of graphennas in transmission. With this purpose, a terahertz signal is driven into the graphenna by means of a pin feed. A simulation study of a graphenna in transmission is performed, which allows obtaining its radiation pattern. The graphenna has a fixed length $L = 5 \mu\text{m}$, while its width takes the values $W = 1, 2$ and $5 \mu\text{m}$ (the geometry for the case $W = 1 \mu\text{m}$ is shown in Fig. 11). The pin feed is located at a distance of $0.1 \mu\text{m}$ from the edge of the graphenna. Fig. 12a shows the radiation pattern of graphennas with the described properties, in the plane parallel to the graphene patch.

Fig. 12b shows the radiation pattern of equivalent metallic antennas, modeled as perfect electric conductor patches of the same dimensions. The radiation pattern is computed at a frequency of 1.3 THz, which approximately corresponds to the resonant frequency of the previously-described graphenna. Even though the metallic antenna is expected to resonate at a higher frequency band, the analysis is performed at the same frequency for the sake of comparison. As it can be seen, in both cases the radiation pattern is similar to that of a half-wave dipole antenna, and the differences between the patterns of graphene and the metallic antennas are minimal.

We therefore conclude that, as it could be expected, future graphennas are not expected to differ significantly with respect to that of equivalent metallic antennas in terms of their radiation pattern.

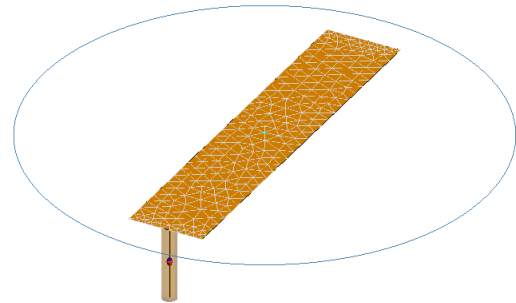


Fig. 11. Schematic diagram of the graphenna in transmission. The graphenna is composed of a graphene patch with a length $L = 5 \mu\text{m}$ and a width $W = 1 \mu\text{m}$, and a pin feed located at $0.1 \mu\text{m}$ from the edge of the graphenna. The blue circle shows the plane in which the radiation diagram is measured.

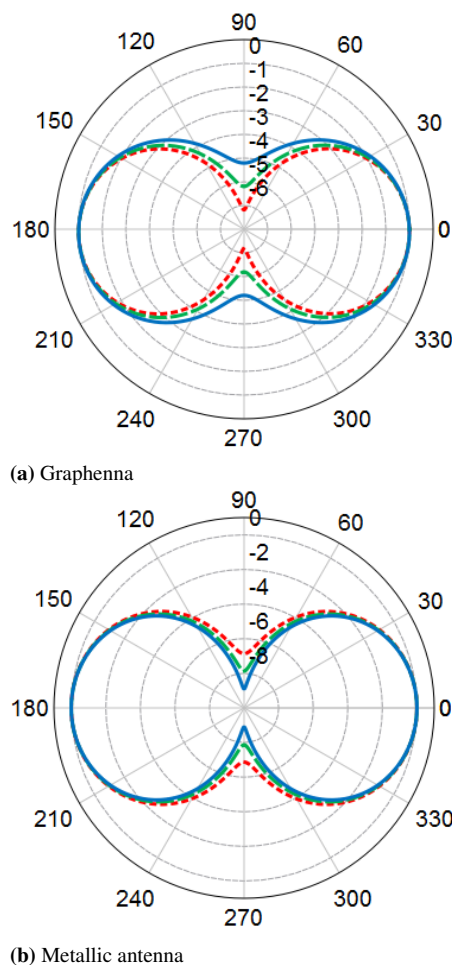


Fig. 12. Radiation pattern of a graphenna (a) and metallic antenna (b) as a function of their width. The plots show the normalized gain in dB, in the plane parallel to the antenna, for an antenna with a length $L = 5 \mu\text{m}$. The results correspond to antenna widths of $W = 1 \mu\text{m}$ (blue solid line), $2 \mu\text{m}$ (green dashed line) and $5 \mu\text{m}$ (red dotted line).

5. Conclusion

Graphene-based plasmonic nano-antennas are envisaged to allow nanosystems to transmit and receive information, creating a novel paradigm known as graphene-enabled wireless communications. In this work, we used a simple model for a graphenna, a rectangular graphene patch based on a dielectric substrate, to perform a parametric study of its radiation properties by means of simulations. The obtained results confirm that a graphenna with dimensions of a few micrometers resonates in the terahertz band, consistently with the theoretical models. Moreover, the dependence of the antenna resonant frequency on several parameters, such as the dimensions of the graphene patch and the dielectric substrate, the chemical potential of graphene and its relaxation time, have been observed. The radiation pattern of a graphenna was found to be very similar to that of an equivalent metallic antenna. These results provide useful guidelines for designers of future graphennas, which will allow the implementation of wireless communications among

nanosystems.

Acknowledgements

This work has been partially supported by the FPU grant of the Spanish Ministry of Education, the German Academic Exchange Service (DAAD) and an ERC Grant (InteGraDe, 307311).

References

- [1] GEIM, A., NOVOSELOV, K. The rise of graphene, *Nature materials*, 2007, vol. 6, no. 3, p. 183 - 191.
- [2] CASTRO NETO, A., GUINEA, F., PERES, N., NOVOSELOV, K., GEIM, A. The electronic properties of graphene. *Reviews of Modern Physics*, 2009, vol. 81, no. 1, p. 109 - 162.
- [3] WU, Y. H., YU, T., SHEN, Z. X. Two-dimensional carbon nanostructures: Fundamental properties, synthesis, characterization, and potential applications. *Journal of Applied Physics*, 2010, vol. 108, 071301.
- [4] SCHWIERZ, F. Graphene transistors. *Nature Nanotechnology*, 2010, vol. 5, no. 7, p. 487 - 496.
- [5] WANG, X., ZHI, L., MÜLLEN, K. Transparent, conductive graphene electrodes for dye-sensitized solar cells. *Nano letters*, 2008, vol. 8, no. 1, p. 323 - 327.
- [6] JORNET, J. M., AKYILDIZ, I. F. Graphene-Based Nano-Antennas for Electromagnetic Nanocommunications in the Terahertz Band. In *European Conference on Antennas and Propagation*, 2010, Barcelona (Spain).
- [7] LEMME, M. C. Current status of graphene transistors. *Solid State Phenomena*, 2010, vol. 156-158, p. 499 - 509.
- [8] WANG, H., HSU, A., WY, J., KONG, J., PALACIOS, T. Graphene-based ambipolar RF mixers. *IEEE Electron Device Letters*, 2010, vol. 31, no. 9, p. 906 - 908.
- [9] PALACIOS, T., HSU, A., WANG, H., Applications of graphene devices in RF communications. *IEEE Communications Magazine*, 2010, vol. 48, no. 6, p. 122 - 128.
- [10] MOON, J., CURTIS, D., ZEHNDER, D., and others Low-Phase-Noise Graphene FETs in Ambipolar RF Applications. *IEEE Electron Device Letters*, 2011, vol. 32, no. 3, p. 270 - 272.
- [11] KOSWATTA, S., VALDES-GARCIA, A., STEINER, M., LIN, Y., AVOURIS, P., Ultimate RF performance potential of carbon electronics. *IEEE Transactions on Microwave Theory and Techniques*, 2011, vol. 59, no. 10, p. 2739 - 2750.
- [12] AKYILDIZ, I. F., BRUNETTI, F., BLÁZQUEZ, C. Nanonetworks: A new communication paradigm. *Computer Networks*, 2008, vol. 52, no. 12, p. 2260 - 2279.
- [13] FREITAS, R. A. Nanotechnology, nanomedicine and nanosurgery. *International Journal of Surgery*, 2005, vol. 3, no. 4, p. 243 - 246.
- [14] TALLURY, P., MALHOTRA, A., BYRNE, L. M., SANTRA, S. Nanobioimaging and sensing of infectious diseases. *Advanced drug delivery reviews*, 2010, vol. 62, no. 4-5, p. 424 - 437.
- [15] FERNANDEZ-PACHECO, R., MARQUINA, C., GABRIEL-VALDIVIA, J., and others Magnetic nanoparticles for local drug delivery using magnetic implants. *Journal of Magnetism and Magnetic Materials*, 2007, vol. 311, no. 1, p. 318 - 322.

- [16] LLATSER, I., KREMERS, C., CABELLOS-APARICIO, A., JORNET, J. M., ALARCÓN, E., CHIGRIN, D. N. Scattering of terahertz radiation on a graphene-based nano-antenna. *AIP Conference Proceedings*, 2011, vol. 1398, p. 144 - 146.
- [17] LLATSER, I., KREMERS, C., CABELLOS-APARICIO, A., JORNET, J. M., ALARCÓN, E., CHIGRIN, D. N. Graphene-based Nano-patch Antenna for Terahertz Radiation", *Photonics and Nanostructures - Fundamentals and Applications*, 2012, vol. 10, no. 4, p. 353 - 358.
- [18] LLATSER, I., KREMERS, C., CHIGRIN, D. N., JORNET, J. M., LEMME, M. C., CABELLOS-APARICIO, A., ALARCÓN, E. Characterization of Graphene-based Nano-antennas in the Terahertz Band. In *Proc. of the Sixth European Conference on Antennas and Propagation*, 2012, Prague (Czech Republic).
- [19] VAKIL, A., ENGHETA, N. Transformation optics using graphene. *Science*, 2011, vol. 332, no. 6035, p. 1291 - 1294.
- [20] FALCOVSKY, L., PERSHOGUBA, S. Optical far-infrared properties of a graphene monolayer and multilayer. *Physical Review B*, 2007, vol. 76, 153410.
- [21] HANSON, G. W. Dyadic Green's functions and guided surface waves for a surface conductivity model of graphene. *Journal of Applied Physics*, 2008, vol. 103, 064302.
- [22] MIKHAILOV, S., ZIEGLER, K. A new electromagnetic mode in graphene. *Physical Review Letters*, 2007, vol. 99, 016803.
- [23] EM Software and Systems, FEKO [Online]. Available: <http://www.feko.info>
- [24] TONGAY, S., BERKE, K., LEMAITRE, M., and others, Stable hole doping of graphene for low electrical resistance and high optical transparency. *Nanotechnology*, 2011, vol. 22, 425701.
- [25] XU, C., JIN, Y., YANG, L., YANG, J., JIANG, X. Characteristics of electro-refractive modulating based on Graphene-Oxide-Silicon waveguide. *Optics Express*, 2012, vol. 20, no. 20, p. 22398 - 22405.
- [26] GEORGE, P. A., STRAIT, J., DAWLATY, J., and others, Ultrafast Optical-Pump Terahertz-Probe Spectroscopy of the Carrier Relaxation and Recombination Dynamics in Epitaxial Graphene. *Nano Letters*, 2008, vol. 8, no. 12, p. 4248 - 4251.
- [27] TRUSHIN, M., SCHLIEMANN, J. Anisotropic photoconductivity in graphene. *EPL*, 2011, vol. 96, 37006.
- [28] HU, J., RUAN, X., CHEN, Y. P. Thermal Conductivity and Thermal Rectification in Graphene Nanoribbons: A Molecular Dynamics Study. *Nano Letters*, 2009, vol. 9, no. 7, p. 2730 - 2735.
- [29] RYZHII, V., RYZHII, M., OTSUJI, T. Negative dynamic conductivity of graphene with optical pumping. *Journal of Applied Physics*, 2007, vol. 101, 083114.